

Comparative Analysis of Förster Resonance Energy Transfer (FRET) in Spherical and Planar Geometries

Onur İNAN^{1*} 

¹Department of Biomedical Device Technology, Bucak Emin Gülmez Technical Sciences Vocational School, Burdur Mehmet Akif Ersoy University, Burdur, Türkiye

ABSTRACT

This research explores the influence of geometric configuration on Förster Resonance Energy Transfer (FRET) efficiency. Specifically, it compares spherical arrangements (relevant to structures like nanoparticles) with planar arrangements (found in systems like cell membranes). A key goal is to clarify the interplay between FRET efficiency, inter-molecular distances, and the characteristic Förster distance. By employing both mathematical models and visual representations, the study seeks to provide a detailed understanding of how FRET operates under these distinct geometric constraints. The findings are intended to be broadly applicable, offering valuable insights for the design and analysis of FRET-based experimental work across diverse scientific disciplines.

Keywords: FRET (Förster Resonance Energy Transfer), Geometric Configuration, Molecular Distance, Simulation

1. INTRODUCTION

Förster Resonance Energy Transfer (FRET), also known in some contexts as Fluorescence Resonance Energy Transfer, is a non-radiative process through which energy is transferred between two fluorophores: a donor and an acceptor. This transfer occurs when the donor molecule, in an excited state, passes its energy to a nearby acceptor molecule without emitting a photon. The mechanism relies on dipole-dipole interactions, which set it apart from traditional radiative energy transfer methods. One of the most distinctive characteristics of FRET is its extreme sensitivity to the distance between the donor and acceptor molecules [1-3].

The efficiency of energy transfer decreases rapidly as the separation distance increases, with the process being most effective when the molecules are within a range of approximately 1 to 10 nanometers. This relationship is described mathematically by the Förster equation, which shows that the transfer efficiency is inversely proportional to the sixth power of the distance between the donor and acceptor [4, 5]. Because of this strong dependence on distance, FRET is often called a "spectroscopic ruler," as it allows researchers to measure nanoscale distances with exceptional precision. The ability of FRET to reveal molecular interactions and spatial arrangements has made it an indispensable tool in fields such as biophysics, molecular biology, and chemistry. Researchers use this technique to investigate dynamic processes, including protein-protein interactions, structural changes in biomolecules, and the assembly of molecular complexes [6, 7].

FRET efficiency, denoted as E , is a quantitative measure representing the proportion of energy transferred from the donor molecule to the acceptor molecule. This efficiency, ranging from 0 (indicating no transfer) to 1 (representing complete transfer), is fundamentally governed by the distance, r , separating the donor and acceptor, and the Förster distance, R_0 , a characteristic parameter unique to each donor-acceptor pair [8, 9].

The relationship is mathematically expressed as: $E = 1 / (1 + (r/R_0)^6)$. The Förster distance, R_0 , signifies the specific separation at which the FRET efficiency reaches 50%. Several factors influence its value: the extent of spectral overlap between the donor's emission and the acceptor's absorption, the relative orientation of the donor and acceptor transition dipoles, and the refractive index of the intervening medium. The Förster distance is calculated using the equation (1). [10]

*Corresponding Author Email: oinan@mehmetakif.edu.tr

Submitted: 26.03.2025 Revision Requested: 23.04.2025 Last Revision Received: 21.05.2025

Accepted: 21.05.2025 Published Online: 23.05.2025



Burdur
Mehmet Akif Ersoy
University Press



Cite this article as: Inan, O. (2025). Comparative Analysis of Förster Resonance Energy Transfer (FRET)

In Spherical and Planar Geometries. Scientific Journal of Mehmet Akif Ersoy University, 8(1): 47-56.

DOI: <https://doi.org/10.70030/simakeu.1665692>

<https://dergipark.org.tr/simakeu>



Content of this journal is licensed under a Creative Commons Attribution-NonCommercial 4.0 International License.

$$R_0^6 = \frac{9000(\ln 10)\kappa^2\phi_D}{128\pi^5 N_A n^4} J(\lambda) \quad (1)$$

Here, κ^2 is the orientation factor, reflecting the relative orientation of the donor emission and acceptor absorption dipoles, typically assumed to be 2/3 for randomly oriented molecules but ranging from 0 to 4. Φ_D represents the quantum yield of the donor in the absence of the acceptor. n is the refractive index of the medium, and N_A is Avogadro's number. The spectral overlap integral, $J(\lambda)$, quantifies the degree of overlap between the donor's normalized fluorescence intensity, $F_D(\lambda)$, and the acceptor's molar extinction coefficient, $\epsilon_A(\lambda)$, and is calculated by equation (2) [11, 12].

$$J(\lambda) = \int_0^{\infty} F_D(\lambda) \epsilon_A(\lambda) \lambda^4 d\lambda \quad (2)$$

Because of its sensitivity to distance, FRET has found widespread applications in various fields (Table 1).

Table 1. Applications of FRET in Various Fields [2, 13-16]

Field	Applications of FRET
Biophysics	Studying protein folding, protein-protein interactions, conformational changes in biomolecules, and membrane dynamics.
Biochemistry Cell Biology	Investigating enzyme kinetics, receptor-ligand binding, and DNA/RNA interactions. Monitoring intracellular signaling pathways, visualizing molecular distributions, and tracking cellular processes.
Nanotechnology Materials Science	Characterizing nanomaterials, developing biosensors, and creating nanoscale devices. Studying polymer blends and self-assembly processes.

While Förster Resonance Energy Transfer (FRET) is widely used in various applications, comparative analyses of how different geometric configurations—specifically spherical versus planar arrangements—affect FRET efficiency are limited. Previous studies have often addressed FRET in spherical or planar contexts, but a direct comparison of these geometries has not been sufficiently explored. This study aims to provide further insights into this area and to understand the geometric influences on FRET efficiency.

This study investigated the intricacies of FRET efficiency. In particular, we examined how the two main geometrical configurations affect it. We focus on two main geometrical configurations in FRET analysis. The research covers two different geometric configurations for FRET analysis. The first configuration examines spherical geometry representing molecular arrangements in various biological and synthetic systems. This geometric framework accommodates donor and acceptor molecules on the spherical surface or distributed within the volumetric domain. Such arrangements are particularly important when studying biological vesicles, micelle structures, spherical nanoparticles, and specific protein complexes that exhibit spherical symmetry. The second geometric configuration involves planar arrangements in which molecular interactions occur along two-dimensional surfaces. This configuration is particularly important in biological systems, especially in studying cellular membranes, surface-fixed molecular assemblies, and layered material architectures. The planar geometry provides a fundamental framework for understanding FRET behavior in systems constrained to two dimensions. This research integrates rigorous mathematical formulations with comprehensive visual representations to develop a detailed understanding of FRET behavior under varying geometric constraints. The findings aim to advance the theoretical framework underlying FRET-based experimental design and data interpretation across diverse scientific applications. This understanding proves particularly valuable for researchers developing new experimental protocols or interpreting complex FRET data in various molecular systems.

2. MATHEMATICAL MODELING: FRAMEWORK AND APPROACH

This section outlines the mathematical underpinnings of our analysis, detailing the methods employed to compute distances and, subsequently, FRET efficiencies within both spherical and planar geometric configurations. Furthermore, it provides a brief overview of the parameter sensitivity analysis conducted to assess the influence of the Förster distance (R_0) on the overall FRET process.

2.1. Spherical Geometry: A Curved Landscape

FRET) efficiency highly depends on the distance, r , between the donor and the acceptor. Accurately determining this distance is critical in calculating FRET efficiency. Using a spherical coordinate system allows for geometrically accurate position determination for distance calculations. In the spherical coordinate system, the distance of the donor molecule from the center is represented by r_d . In the simplest case, if both donor and acceptor are located on the sphere's surface, r_d is directly equal to the sphere's radius. However, if the donor molecule is located at a different distance from the center, r_d can also express this distance. Similarly, we define the distance of the acceptor from the center by r_a . Besides distances, angles must also be taken into account. The polar angle θ measures the angular separation between the donor and the acceptor, and this angle is determined when viewed from the center of the sphere. The angle θ varies between 0 and π radians (180 degrees). Another angle, the azimuthal angle ϕ , defines the projection of the donor and acceptor positions on the "equator" (xy -plane). This angle is measured from the positive x -axis and ranges from 0 to 2π radians (360 degrees). These angles and distances are necessary for an accurate calculation of FRET efficiency, and these calculations play a critical role in determining the efficiency of energy transfer.

Using the values of r_d , r_a , θ and ϕ , a special version of the cosine law adapted to spherical coordinates can calculate the distance (r) between donor and acceptor. This gives the precise separation needed for FRET calculations.

This adaptation is crucial because it accounts for the inherent curvature of the spherical geometry.

$$r = \sqrt{r_d^2 + r_a^2 - 2r_d r_a \cos \gamma} \quad (3)$$

Where γ represents the central angle between the donor and acceptor position vectors, it is calculated using equation (2).

$$\cos \gamma = \cos \theta_d \cos \theta_a + \sin \theta_d \sin \theta_a \cos(\phi_d - \phi_a) \quad (4)$$

In the simplified case where both donor and acceptor are on the surface of a sphere with radius R , and only concerned with the angle between them, the distance equation simplifies to equation (3). If only given a single angle, equation (5) becomes equation (3).

$$r = \sqrt{2R^2(1 - \cos \gamma)} = 2R \sin(\gamma / 2) \quad (5)$$

Once the distance, r , is determined, the FRET efficiency, E , is calculated using the standard Förster equation.

2.2. Planar Geometry

Planar geometry deals with donor and acceptor molecules on a flat, two-dimensional plane. This applies to systems such as cell membranes or surface-fixed molecules. The distance, r , between the donor and acceptor is calculated using the Pythagorean theorem in Cartesian coordinates (equation 6). Here, x , y , and z represent the Cartesian coordinates for the donor and acceptor molecules.

$$r = \sqrt{(x_d - x_a)^2 + (y_d - y_a)^2 + (z_d - z_a)^2} \quad (6)$$

The FRET efficiency is calculated using the same Förster equation as the spherical geometry.

2.3. Parameter Sensitivity Analysis

A parameter sensitivity analysis was performed to understand the impact of the Förster distance R_0 on FRET efficiency:

1. **Varying R_0 :** Systematically changing the value of R_0 within a relevant range (e.g., from 5 nm to 15 nm).
2. **Calculating E :** For each R_0 value, we calculate the FRET efficiency, E , as a function of distance, r , using the appropriate distance equation for the chosen geometry (spherical or planar).

3. **Plotting E vs. r:** Plotting E versus r for different values of R_0 allows one to visualize how the efficiency-distance relationship changes with R_0 .
4. **Logarithmic Scale Analysis:** Plotting the relationship between distance and FRET efficiency on a logarithmic scale helps highlight the efficiency behavior at very short and very long distances and better visualize the steepness of efficiency declines.
5. **Orientation Factor (κ^2):** While often assumed to be $2/3$ (for dynamic random averaging), it's important to acknowledge that the orientation factor can significantly impact R_0 and thus FRET efficiency. A brief discussion of κ^2 and its potential influence could be included, although a full analysis of κ^2 is beyond the scope of this basic model.

This systematic approach allows us to quantitatively assess the sensitivity of FRET efficiency to changes in the Förster distance and to understand the implications for interpreting FRET measurements.

3. RESULTS AND DISCUSSION

This section presents and discusses the results of the FRET efficiency calculations for both spherical and planar geometries, highlighting the key differences and the underlying reasons for these differences.

3.1. Spherical Geometry

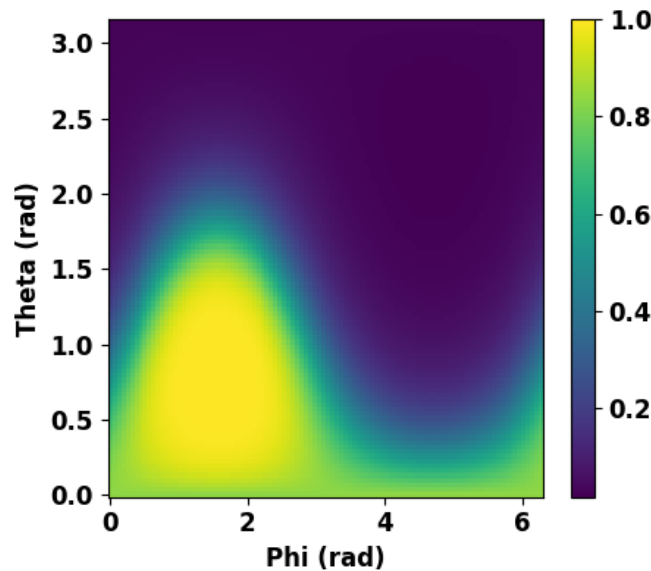


Fig 1. FRET Efficiency (2D Heat Map)

The 2D heat map (Figure 1) visualizes FRET efficiency as a function of the azimuthal angle (ϕ) and the polar angle (θ). Crucially, maximum FRET efficiency doesn't occur uniformly but is localized to specific combinations of ϕ and θ . This indicates a strong angular dependence. As θ increases (moving from the "pole" towards the "equator" of the sphere), the distance, r , between the donor and acceptor generally increases, leading to a decrease in FRET efficiency. The color gradient of the heat map (e.g., from yellow for high efficiency to purple for low efficiency) directly reflects this distance-dependent change.

The 3D surface plot (Figure 2) represents the same data's three-dimensional representation. The "wave-like" pattern is a direct visual consequence of the angular dependence of the distance, r , and consequently, the FRET efficiency, E . The symmetry observed along the azimuthal axis (ϕ) is expected, especially when r_d and r_a are constant, as rotating the system around the z-axis (changing ϕ) doesn't change the *relative* distance between donor and acceptor if their θ values are fixed.

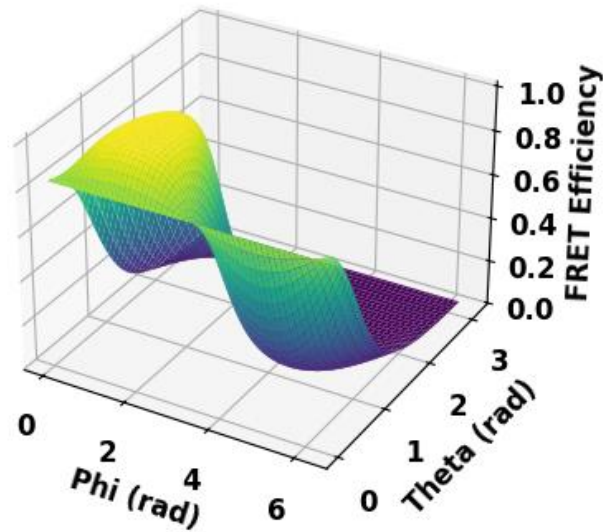


Fig 2. FRET Efficiency (3D Surface Plot)

By taking a cross-section of the 3D surface plot at a fixed ϕ (e.g., $\phi = \pi$), we obtain a 2D plot of FRET efficiency versus θ (Figure 3). This plot demonstrates the monotonic decrease in FRET efficiency as θ increases. This monotonic decrease is a direct consequence of the inverse sixth-power relationship between distance and FRET efficiency in the Förster equation. As θ increases, r increases, and E decreases rapidly.

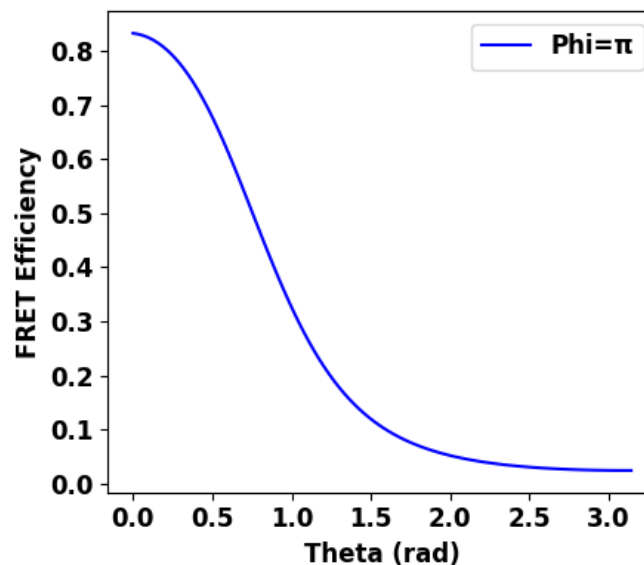


Fig 3. FRET Efficiency vs. θ (Cross-section)

The curvature inherent in spherical geometry is the primary reason for the observed FRET efficiency patterns. Even small angular separation (θ) changes can significantly change the distance, r , between the donor and acceptor. This makes FRET efficiency highly sensitive to the angular configuration in spherical systems. The symmetry along the azimuthal angle (ϕ), when r_d and r_a are constant, simplifies the analysis somewhat, but the fundamental angular dependence remains.

3.2. Planar Geometry

The 2D heat map (Figure 4) for planar geometry shows FRET efficiency as a function of the donor and acceptor positions on the X-Y plane. The maximum FRET efficiency is observed at the plane's center (assuming the acceptor is

fixed at the origin), where the donor and acceptor are closest. As we move radially outward from the center, the distance, r , increases, and the FRET efficiency decreases. The color gradient reflects this radial decrease.

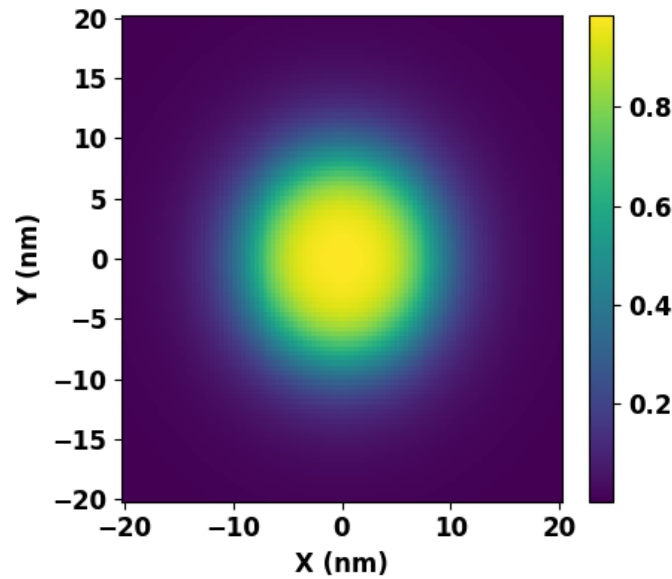


Fig 4. FRET Efficiency (2D Heat Map)

The 3D surface plot (Figure 5) shows a peak at the center, corresponding to the minimum donor-acceptor distance. The efficiency decreases symmetrically in all directions, reflecting the isotropic nature of the plane. The spherical geometry has no wave-like patterns because there's no angular dependence; the efficiency depends solely on the radial distance.

A cross-section of the 3D surface plot (Figure 6) along the X-axis (with Y fixed, e.g., $Y = 0$) shows the FRET efficiency as a function of the X-coordinate. The efficiency is highest at $X = 0$ (where the donor is closest to the acceptor) and decreases symmetrically as the donor moves away from the center along the X-axis. This symmetry is a direct consequence of the linear distance relationship in planar geometry.

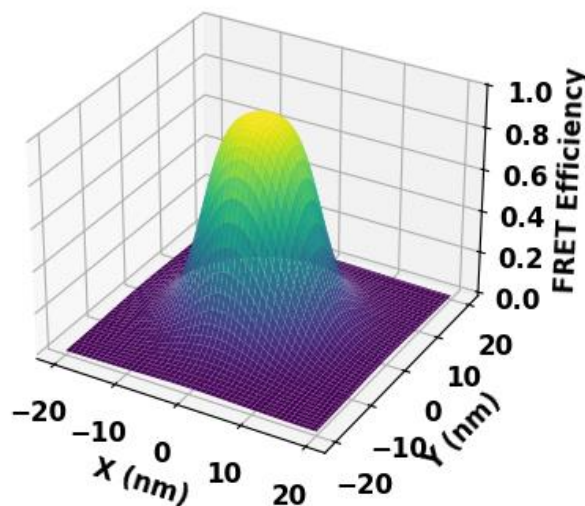


Fig 5. FRET Efficiency (3D Surface Plot)

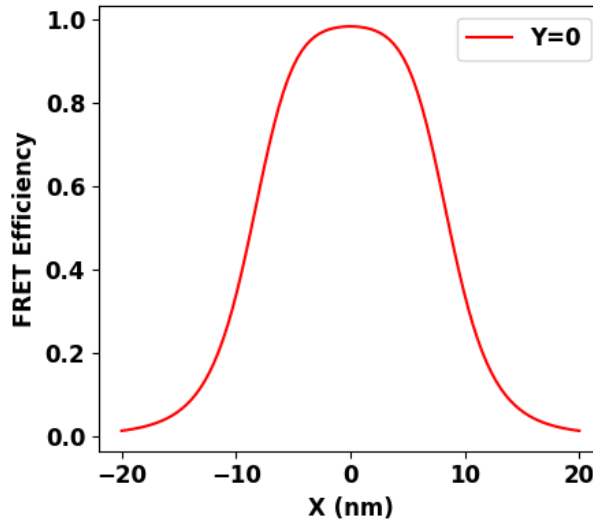


Fig 6. FRET Efficiency vs. X (Cross-section)

The absence of curvature in planar geometry is the key factor influencing FRET efficiency. The distance between the donor and acceptor is a simple, linear function of their Cartesian coordinates, leading to symmetric and predictable efficiency patterns. There are no angular dependencies; the FRET efficiency is solely a function of the Cartesian distance, r .

3.3. Parameter Analysis

Figure 7 shows how FRET efficiency varies depending on the distance between donor and acceptor. In Figure 7.a, the Y axis shows the FRET efficiency, and the X axis shows the distance (in nm). In this graph, the blue line represents $R_0=8$ nm, the orange line $R_0=10$ nm, and the green line $R_0=12$ nm. The blue line starts at 1.0000 and decreases to approximately 0.99975 at 20 nm, while the orange line decreases from 1.0000 to 0.99985, and the green line decreases from 1.0000 to 0.99995. This shows that the FRET efficiency of lower R_0 values decreases more rapidly at shorter distances. Figure 7.b presents the relationship between distance and FRET efficiency on a logarithmic scale. The Y-axis again shows FRET efficiency, while the X-axis shows distance on a logarithmic scale. This graph's blue, orange, and green lines represent $R_0=8$ nm, $R_0=10$ nm, and $R_0=12$ nm, respectively. The blue line shows a sharp decrease at about 15 nm starting at 1.0000, while the orange line shows a similar but less pronounced decrease. The green line shows less change with increasing distance, allowing the efficiency to remain more constant. It emphasizes that FRET efficiency decreases more rapidly at shorter distances and that higher R_0 values tend to keep the efficiency more constant.

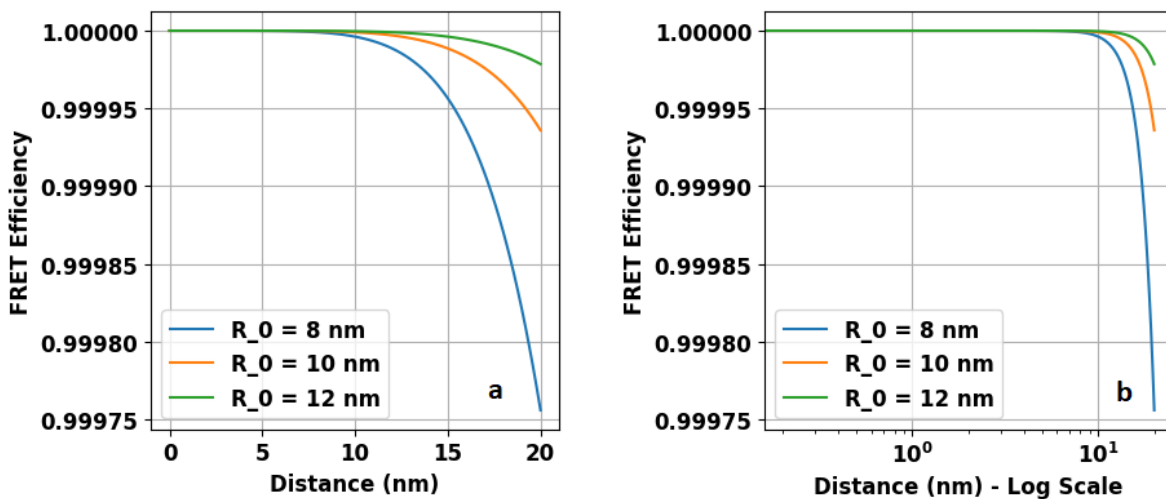


Fig 7. FRET efficiency versus distance

3.4. Comparison of Spherical and Planar Geometries

The following table summarizes the key differences between spherical and planar geometries:

Table 1. Comparison of Spherical and Planar Geometries

Aspect	Spherical Geometry	Planar Geometry
Distance Calculation	Depends on angular separation (θ , and potentially ϕ) and curvature. The relationship between distance and angle is non-linear.	Depends linearly on Cartesian coordinates (x , y , and potentially z). The relationship between distance and coordinates is linear.
Efficiency Patterns	Exhibits angular dependence. Efficiency is not uniform and shows a wave-like pattern in 3D plots. Symmetry may exist along the azimuthal angle (ϕ) under certain conditions.	Exhibits radial symmetry. Efficiency decreases uniformly as distance from the acceptor increases. No angular dependence.
Sensitivity	Highly sensitive to small changes in angular separation, especially near the poles.	Uniform sensitivity across the plane. Changes in distance result in predictable changes in efficiency.
Complexity	More complex due to the non-linear relationship between distance and angle. Requires careful consideration of angular coordinates.	Simpler due to the linear relationship between distance and coordinates.
Applications	Vesicles, micelles, spherical nanoparticles, and protein complexes with curved surfaces.	Cell membranes, surface-immobilized molecules, layered materials.

This study quantitatively demonstrates that FRET efficiency behaves nonlinearly in spherical systems due to angular dependence, while in planar systems, there is a predictable relationship with radial distance. Saini et al. [18] emphasize that the assumptions of Förster theory are limited in large conjugated structures, metal nanoparticles, and polymer systems. Both studies recognize the critical importance of the Förster distance parameter: The current research examines the practical implications of its optimization, while Saidi's analysis shows that this parameter can be affected by geometry and environmental factors. Non-spherical structures and orientation dynamics indicate that the theoretical models in both studies require revision. In conclusion, geometric design and theoretical model selection in FRET-based systems should be optimized to achieve consistent results from nanomaterials engineering to biophysical applications.

Oliden-Sánchez et al. [19] show that organic chromophores (DMAN, rhodamine 123, Nile Blue) entrapped in a rigid aluminophosphate matrix provide emission in the entire visible spectrum by energy transfer via FRET. The one-dimensional extra-wide channels of the IFO-type zeolitic structure allow the confinement of bulky dyes, while the fixation of the D-A pairs in the rigid matrix facilitates the control of geometrical parameters. While this study investigates its optimization as geometry-dependent, this work shows how it can be used in practice with optimized D-A pairs in a rigid matrix. In conclusion, this study models the fundamental effects of geometry on FRET, while this work presents a feasible way to improve FRET efficiency through material design. The two approaches can complement the development of FRET-based materials in controlled geometries.

Grzedowsk et al. [20] have demonstrated how DNA nanocube structures can manipulate FRET signals in a geometrically optimized system with molecular level control on the gold surface. DNA nanocubes' self-organizing monolayer (SAM) allows the inter-fluorophore distance to be fixed with the nanocube dimensions, minimizing the angular dependence problem in this study. This rigid structure allows for a controlled decrease or increase of the FRET signal during target DNA hybridization, similar to the predictable FRET behavior in planar systems. It emphasizes the critical role of geometry in FRET-based biosensor design with different dimensions. The geometrical optimization obtained at the end of this study may prove indispensable for understanding fundamental FRET dynamics and developing practical biosensor applications.

4. CONCLUSION

This study systematically explores the interplay between geometry and FRET efficiency, revealing critical insights into energy transfer dynamics in spherical and planar systems. The key conclusions are as follows:

Geometric Influence on FRET Efficiency: In spherical geometries, FRET efficiency exhibits strong angular dependence due to the nonlinear relationship between donor-acceptor distance and polar angle (θ). The sphere's curvature amplifies sensitivity to angular displacements, with efficiency declining sharply as θ increases (e.g., from the pole to the equator). The observed wave-like patterns in 3D plots and azimuthal symmetry underscore the complexity introduced by spherical curvature. FRET efficiency depends solely on radial distance in planar geometries, resulting in radially symmetric patterns. The absence of angular dependence simplifies the relationship, with efficiency decreasing predictably as donors move away from the acceptor. This linearity contrasts starkly with the nonlinear behavior in spherical systems.

Role of Förster Distance (R_0): The parameter analysis highlights R_0 as a critical determinant of FRET efficiency. Smaller R_0 values (e.g., 8 nm) lead to a rapid decline in efficiency at shorter distances, while larger R_0 values (e.g., 12 nm) extend the effective energy transfer range. This emphasizes the importance of selecting donor-acceptor pairs with R_0 tailored to the system's spatial constraints.

Sensitivity and Applications: Spherical systems (e.g., vesicles, nanoparticles) demand careful consideration of angular configurations, as small positional changes near the poles significantly alter efficiency. This sensitivity may limit FRET reliability in highly curved environments unless spatial constraints are well-characterized.

Planar systems (e.g., cell membranes) offer greater predictability due to radial symmetry, making them ideal for quantitative studies where distance is the primary variable.

Practical Implications: These findings underscore the necessity of accounting for geometry when designing FRET-based experiments or interpreting data. For instance, spherical geometries may require advanced modeling to disentangle angular effects, while planar systems benefit from straightforward distance calibration. Additionally, the R_0 -dependent efficiency profiles suggest that optimizing the donor-acceptor pair's Förster radius can enhance resolution in targeted applications, such as biosensing or molecular imaging.

By bridging theoretical models with geometric realities, this work provides a framework for improving the accuracy of FRET measurements across diverse nanoscale and biological systems. Future studies could extend these principles to hybrid geometries or dynamic systems where curvature and donor-acceptor mobility evolve over time.

ORCID

Onur İNAN  <https://orcid.org/0000-0003-4573-7025>

REFERENCES

- [1]. Clegg, R. M. (2009). Förster resonance energy transfer—FRET what is it, why do it, and how it's done. *Laboratory techniques in biochemistry and molecular biology*, 33, 1-57.
- [2]. Kaur, A., Kaur, P., & Ahuja, S. (2020). Förster resonance energy transfer (FRET) and applications thereof. *Analytical Methods*, 12(46), 5532-5550.
- [3]. Szabó, Á., Szöllösi, J., & Nagy, P. (2022). Principles of resonance energy transfer. *Current protocols*, 2(12), e625.
- [4]. Chen, G. (2005). *Nanoscale energy transport and conversion: a parallel treatment of electrons, molecules, phonons, and photons*. Oxford University Press.
- [5]. Metz, S., & Marian, C. M. (2025). Computational Approach to Phosphor-Sensitized Fluorescence Based on Monomer Transition Densities. *Journal of Chemical Theory and Computation*, 21(5), 2569-2581.

- [6]. Nüesch, M., Ivanović, M. T., Nettels, D., Best, R. B., & Schuler, B. (2025). Accuracy of distance distributions and dynamics from single-molecule FRET. *Biophysical Journal*.
- [7]. Loidolt-Krüger, M. (2025). Perspective: fluorescence lifetime imaging and single-molecule spectroscopy for studying biological condensates. *Methods in Microscopy*, (0).
- [8]. Berney, C., & Danuser, G. (2003). FRET or no FRET: a quantitative comparison. *Biophysical journal*, 84(6), 3992-4010.
- [9]. Shrestha, D., Jenei, A., Nagy, P., Vereb, G., & Szöllösi, J. (2015). Understanding FRET as a research tool for cellular studies. *International journal of molecular sciences*, 16(4), 6718-6756.
- [10]. Zhou, M., Zhang, K., Li, X., Ge, Y., Zhang, W., Lu, P., & Hao, X. (2024). Improved Exciton Diffusion through Modulating Förster Resonance Energy Transfer for Efficient Organic Solar Cells. *Solar RRL*, 8(13), 2400136.
- [11]. Wong, K. F., Bagchi, B., & Rossky, P. J. (2004). Distance and orientation dependence of excitation transfer rates in conjugated systems: beyond the Förster theory. *The Journal of Physical Chemistry A*, 108(27), 5752-5763.
- [12]. Patterson, G. H., Piston, D. W., & Barisas, B. G. (2000). Förster distances between green fluorescent protein pairs. *Analytical biochemistry*, 284(2), 438-440.
- [13]. Fang, C., Huang, Y., & Zhao, Y. (2023). Review of FRET biosensing and its application in biomolecular detection. *American journal of translational research*, 15(2), 694.
- [14]. Gopal, A. R., Joy, F., Dutta, V., Devasia, J., Dateer, R., & Nizam, A. (2024). Carbon dot-based fluorescence resonance energy transfer (FRET) systems for biomedical, sensing, and imaging applications. *Particle & Particle Systems Characterization*, 41(1), 2300072.
- [15]. Liu, C. (2024, January). Application of FRET and TBET in bioimaging and biosensors. In *Third International Conference on Biological Engineering and Medical Science (ICBioMed2023)* (Vol. 12924, pp. 346-353). SPIE.
- [16]. Kaur, A., & Dhakal, S. (2020). Recent applications of FRET-based multiplexed techniques. *TrAC Trends in Analytical Chemistry*, 123, 115777.
- [17]. Medintz, I. L., & Hildebrandt, N. (Eds.). (2013). *FRET-Förster resonance energy transfer: from theory to applications*. John Wiley & Sons.
- [18]. Saini, S., Srinivas, G., & Bagchi, B. (2009). Distance and orientation dependence of excitation energy transfer: from molecular systems to metal nanoparticles. *The Journal of Physical Chemistry B*, 113(7), 1817-1832.
- [19]. Oliden-Sánchez, A., Sola-Llano, R., Pérez-Pariente, J., Gómez-Hortigüela, L., & Martínez-Martínez, V. (2024). Exploiting the photophysical features of DMAN template in ITQ-51 zeotype in the search for FRET energy transfer. *Physical Chemistry Chemical Physics*, 26(2), 1225-1233.
- [20]. Grzedowski, A. J., Jun, D., Mahey, A., Zhou, G. C., Fernandez, R., & Bizzotto, D. (2024). Engineering DNA Nanocube SAM Scaffolds for FRET-Based Biosensing: Interfacial Characterization and Sensor Demonstration. *Journal of the American Chemical Society*, 146(46), 31560-31573.